

### Results and Discussion:

#### *Melt occurrence as a function of crater size and morphology.*

Impact melt is more common at fresh simple craters ( $D < \sim 15$  km) than has previously been thought. The smallest extensively studied crater with interior melt is 750 m in diameter, but we have noted the occurrence of even smaller melt-containing craters. At very small craters ( $D < 2$  km), impact melts typically occur as narrow ponds of low-albedo material on crater floors, less common dark streaks on walls, and very thin discontinuous veneers around the rim crests. The melt deposits associated with slightly larger simple craters ( $D = 2-7$  km) are similar but more abundant than those at smaller craters. Shallow ponds often occur among the small floor hummocks, and hard-rock veneers cover much of the crater floors. It appears that some of the melt flowed onto the floor from the lower portions of the crater walls and embayed clastic debris emplaced by mass wasting from the crater walls. Though some minor wall failure has occurred at craters in this size range, the positions of these craters on depth-diameter plots indicate that there has been very little, if any, reduction in depth [8-10].

Interior melt volumes are quite variable in fresh craters from 7 to 12 km in diameter. These deposits range from unobserved or present in only trace amounts to quite abundant. Extensive deposits of exterior melt are first observed around craters near the upper limit of this size range [6,8].

Numerous workers have documented the changes in lunar crater morphology and morphometry, which start at a diameter of about 15 km as smaller, simple craters undergo a transition to larger, complex craters that exhibit central peaks and wall terraces [e.g., 9,10]. It appears that the crater modification processes operative at craters between 15 and 25 km in diameter influence melt deposit morphologies and abundances. While most fresh primary craters in this diameter range for which adequate photography exists do contain at least some melt, the amounts are extremely variable. Dawes ( $D = 17$  km) is typical of craters in this size range. Significant accumulations of impact melt are restricted to a small area immediately east of the central peak [7]. Additional melt was probably present initially but was buried by scallop material slumped onto the crater floor during the modification stage of the impact cratering event. Fresh craters in this size range that exhibit little or no interior melt are generally characterized by the presence of extensively scalloped walls and/or swirl-textured floors, features indicative of pervasive wall failure [7,8]. The results of our analysis of the interior morphologies of these craters indicate that much of the interior melt was totally buried by scallop material. We conclude that the variable amounts of interior melt associated with craters in this size range can best be explained by differences in the degree and style of wall failure.

Fresh impact craters over 25-30 km in diameter are extensively modified and exhibit terraced walls, central peaks, and flat floors with abundant deposits of impact melt. Wall failure has been more extensive and deep-seated at the larger terraced-walled craters, and little melt appears to have been buried during the modification stage. The results of detailed mapping of interior and exterior melt distributions indicate that ponded material becomes relatively more abundant on the floors and rims of these larger craters [8].

*Exterior melt volumes as a function of crater diameter.* Previous work has emphasized the role of oblique impact and preexisting topography in controlling the distribution and amounts of exterior melts [5,6,8]. While it is clear that these factors do cause variable amounts of melt to be emplaced on crater rims, a variety of evidence indicates that relatively greater quantities of melt are present on the

rims of larger craters: (1) the dominance of large exterior melt ponds over flows and hard-rock veneer at craters over 50 km in diameter [6,8]; (2) the tendency for melts to occur at greater distances from the parent craters as a function of crater size; (3) the observation that exterior melt ponds are larger and more widespread at larger craters; and (4) quantitative estimates of melt volumes, which indicate that relatively more melt is present on the rims of larger structures. Even so, this may not imply that a greater percentage of the total melt has been ejected since the total amount of melt generated was also relatively greater at larger structures [8].

*Interior melt volumes as a function of crater diameter.* There also appears to be a systematic variation in the amounts of molten material in crater interiors. Since the extent and thicknesses of the ponded material on crater floors tend to increase as a function of crater size, more melt may be present in the interiors of larger craters. Support is provided by quantitative estimates of interior melt volumes for specific craters where detailed topographic data exist [11,12]. A similar trend has been noted for the impact melt volumes associated with terrestrial impact structures [13,14].

*Influence of substrate on melt generation.* Numerous cratering studies have demonstrated the importance of target characteristics in determining the morphology of lunar craters [e.g., 15,16]. Therefore, we made an attempt to determine the influence of substrate on the relative amounts of impact melt associated with craters in highland vs. mare terrains. A comparison of the mapped interior melt deposits in similar-sized craters ( $D < 50$  km) suggests that highland craters contain melts in amounts either equal to or less than the amounts present in mare craters. This observation does not necessarily indicate that more melt was generated by impact into mare targets. The observation could be explained by one or more of the following: (1) for a given impact energy, larger craters may be formed in the highlands relative to the mare; (2) the style and degree of wall failure is known to be dependent on terrain, topography, and substrate [15]; and (3) a limited amount of evidence suggests that more melt was ejected from highland craters.

**References:** [1] Simonds C. et al. (1976) *Am. Mineral.*, 61, 569. [2] Simonds C. et al. (1977) *Proc. LSC 8th*, 1869. [3] Taylor S. R. (1982) *Planetary Science: A Lunar Perspective*, 481 pp. [4] Spudis P. et al. (1991) *Proc. LPSC, Vol. 21*, 151. [5] Howard K. and Wilshire H. (1975) *J. Res. U.S. Geol. Survey*, 3, 237. [6] Hawke B. and Head J. (1977) *Impact and Explosion Cratering*, 815. [7] Hawke B. and Head J. (1977) *LSC VIII*, 415. [8] Hawke B. and Head J. (1979) *LPSC X*, 510. [9] Wood C. and Andersson L. (1978) *Proc. LPSC 9th*, 3669. [10] Pike R. (1977) *Impact and Explosion Cratering*, 489. [11] Lange M. and Hawke B. (1979) *Conf. Lunar Highlands Crust*, 99. [12] Lange M. and Hawke B. (1980) *Proc. LPSC 10th*, 599. [13] Dence M. et al. (1977) *Impact and Explosion Cratering*, 247. [14] Grieve R. et al. (1977) *Impact and Explosion Cratering*, 791. [15] Cintala M. et al. (1977) *Proc. LSC 8th*, 3409. [16] Head J. (1976) *Proc. LSC 7th*, 2913.

**LARGE IMPACTS IN THE BALTIC SHIELD WITH SPECIAL ATTENTION TO THE UPPLAND STRUCTURE.** H. Henkel and R. Lilljequist, Institute for Fotogrammetry, KTH, S-10044 Stockholm and Department of Geology, University of Stockholm, S-106 91, Stockholm, Sweden.

Within the Baltic Shield several very large structures have been identified and are suspected to be of meteorite impact origin (Fig. 1 and Table 1). Some of these deeply eroded circular features will be

537-46N 93-4201 40 3 475184

53187283



Fig. 1. Craterform structures in Fennoscandia. Numbers 45, 46, and 55 are large suspected impact structures.

TABLE 1. Location and indication features of large circular structures in Fennoscandia (compare Fig. 1).

No	Name	Lat/N	Lat/E	Indication	Diameter	Age
45	Uppland	60.0	17.0	Top., Grav.	320	Proterozoic
46	Nunjes	69.2	20.5	Grav., Magn.	200	Proterozoic
55	Marras	66.9	25.2	Top., Grav., Magn	160	Proterozoic

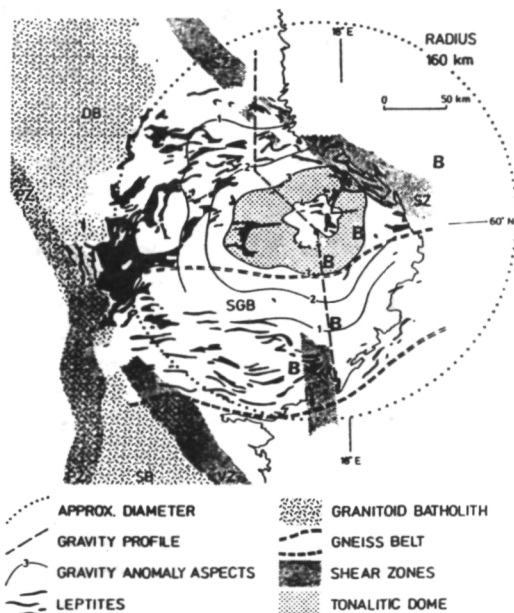


Fig. 2. Uppland structure. SGB = Sormland Gneiss Belt; SZ = Singö Shear Zone; PZ = Protogin Zone; VZ = Västerås Shear Zone; DB = Dala Batholiths; SB = Småland Batholiths; B = breccia dyke occurrences.

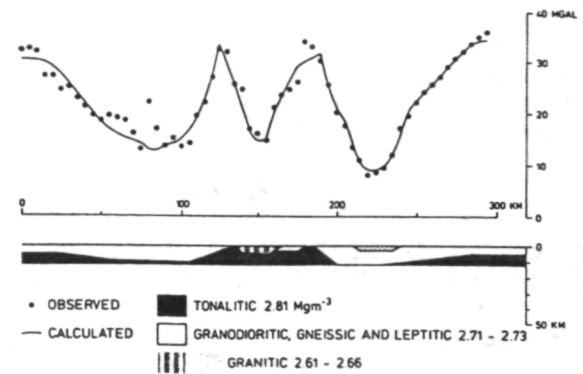


Fig. 3. Gravity profile of the Uppland structure.

presented with special attention to the Uppland structure, where several indications point toward an impact origin in the mid-Proterozoic. The structures exceed 100 km in diameter and the topographic expression is inferior or absent. An arcuate arrangement of lithologies occurs around the margin of the structures and the central regions show conform magnetic and positive gravity anomalies.

The Uppland structure (Fig. 2) is approximately 320 km in diameter as expressed by morphological, geological, and geophysical concentric patterns. The central part is topographically remarkably flat and is characterized by an unusual irregular fracture pattern. A subcircular central tonalite with density of  $2.81 \text{ Mg}^{-3}$  gives a positive gravity anomaly of 35 mgal and the gravimetric profile is very similar to that of Manicouagan and Vredefort. The tonalite constitutes a huge antiform, 80 km in diameter, probably representing a 12-km structural uplift of infracrustal rocks (Fig. 3). The flanks of the tonalite are characterized by recrystallized pseudotachylitic breccia dykes and breccia zones. Around the central parts amphibolite-grade metamorphic rocks appear as large fragments within a fine-grained granite interpreted as a thermally annealed melt rock. Several occurrences of breccia dykes and breccia-bearing melts have been identified about 100 km from the gravimetric center of the structure. Outside the melting ring, downslided and eroded crater wall rocks of high metamorphic grade (garnet-bearing gneisses and migmatites) occupy most of the terrain. The northwestern quadrant has later been downfaulted and preserves less metamorphic rocks of mainly sedimentary origin and a large quantity of iron deposits and Zn-bearing sulphide mineralizations within huge hydrothermal fields. The northeastern quadrant is affected by a broad shear zone (the Singö Zone) and Rapakivi-type intrusives. The southern sector is overprinted by an east-west striking shear zone (the Sormland Gneiss Zone).

Impact-related ore deposits are located around the margin of the structure and are interpreted as preexisting downfaulted iron formations, and deposits formed from remobilization of these preimpact occurrences. The so-called ball ores are interpreted to have formed by fluid injection similar to the formation of breccia dykes. The extensive hydrothermal alteration along the outer margin of the structure have created extreme soda and K-enriched rocks ("leptites") from preexisting gneiss granites and supracrustal sedimentary gneisses. As an example, magnetite-skarn deposits are formed within gneiss granites in hydrothermal cells created during the postimpact phase.

The other two suspected large impact structures (Fig. 1) have central gravity highs and conformally arranged occurrences of metasedimentary rocks (greenstones) along parts of their periphery, here interpreted as parts of a subsided ring basin. No candidate for a melt rock has so far been identified in those structures.

**THE PANTHER MOUNTAIN CIRCULAR STRUCTURE, A POSSIBLE BURIED METEORITE CRATER.** Y. W. Isachsen<sup>1</sup>, S. F. Wright<sup>2</sup>, F. A. Revetta<sup>3</sup>, and R. J. Dineen<sup>4</sup>, <sup>1</sup>New York State Geological Survey, <sup>2</sup>University of Vermont, <sup>3</sup>SUNY College at Potsdam, <sup>4</sup>Roy F. Weston Company.

Panther Mountain, located near Phoenicia, New York, is part of the Catskill Mountains, which form the eastern end of the Allegheny Plateau in New York. It is a circular mass defined physiographically by an anomalous circular drainage pattern produced by Esopus Creek and its tributary Woodland Creek. The mountain is 10 km in diameter and has a maximum relief of 860 m. It is well displayed on Landsat images and aerial photographs. Pervasive fluvial cross-bedding made it impossible to determine whether the structure is slightly domical, slightly basinal, or unwarped. The circular valley that rings the mountain is fracture-controlled; where bedrock is exposed, it shows a joint density 5 to 10 times greater than that on either side of the valley. Where obscured by alluvial valley fill, the bedrock's low seismic velocity suggests that this anomalous fracturing is continuous in the bedrock underlying the rim valley.

North-south and east-west gravity and magnetic profiles were made across the structure. Terrain-corrected, residual gravity profiles show an 18-mgal negative anomaly, and very steep gradients indicate a near-surface source. Several possible explanations of the gravity data were modeled. Only one of the computed profiles matched the measured values, namely that of a shallowly buried meteorite crater with a diameter of 10 km and a breccia lens 3 to 4 km deep, which would pass through the entire Paleozoic section and perhaps into the crystalline basement. The closely spaced joints in the rim valley are interpreted as the result of differential compaction over the inferred crater rim, leading to bending and dense fracturing of the bedrock. The magnetic profiles show only small variations in intensity over the Panther Mountain area. This is not surprising in view of the significant depth to basement rocks (~3 km) and the low content of ferromagnetic minerals in the overlying Paleozoic section. Regional fracture-controlled linear valleys north and south of Panther Mountain terminate at the rim valley. This is consistent with the inferred breccia lens beneath the structure, which would absorb rather than transmit stresses propagated upward from the basement.

We conclude that the Panther Mountain circular structure is probably a buried meteorite crater that formed contemporaneously with marine or fluvial sedimentation during Silurian or Devonian time. An examination of drill core and cuttings in the region is now underway to search for ejecta deposits and possible seismic and tsunami effects in the sedimentary section. Success would result in both dating the impact and furnishing a chronostratigraphic marker horizon.

AA54/527 P. 2 475186  
539 = 46 N93-10151  
**GEOMECHANICAL MODELS OF IMPACT CRATERING: PUCHEZH-KATUNKI STRUCTURE.** B. A. Ivanov, Institute for Dynamics of Geospheres, Russian Academy of Science, Leninsky Prospect, 38, corp.6, Moscow 117979, Russia.

Impact cratering is a complex natural phenomenon that involves various physical and mechanical processes [1]. Simulating these processes may be improved using the data obtained during the deep drilling at the central mound of the Puchezh-Katunki impact structure [2].

A research deep drillhole (named Vorotilovskaya) has been drilled in the Puchezh-Katunki impact structure (European Russia, 57°06'N, 43°35'E). The age of the structure is estimated at about 180 to 200 m.y. [1]. The initial rim crater diameter is estimated at about 40 km. The central uplift is composed of large blocks of crystalline basement rocks. Preliminary study of the core shows that crystalline rocks are shock metamorphosed by shock pressures from 45 GPa near the surface to 15–20 GPa at a depth of about 5 km [2]. The drill core allows the possibility of investigating many previously poorly studied cratering processes in the central part of the impact structure.

As a first step one can use the estimates of energy for the homogeneous rock target. The diameter of the crater rim may be estimated as 40 km. The models elaborated earlier [cf. 3] show that such a crater may be formed after collapse of a transient cavity with a radius of 10 km. The most probable range of impact velocities from 11.2 to 30 km/s may be inferred for the asteroidal impactor. For the density of a projectile of 2 g/cm<sup>3</sup> the energy of impact is estimated as 1E28 to 3E28 erg (or about 500,000 Mton TNT).

In the case of vertical impact, the diameter of an asteroidal projectile is from 1.5 to 3 km for the velocity range from 11 to 30 km/s. For the most probable impact angle of 45°, the estimated diameter of an asteroid is slightly larger: from 2 to 4 km.

For the homogeneous rock target one may expect 40 cubic km of impact melt. The depth of such a melt zone is about 3 km, so two-thirds of the probable depth of a melt zone seems to be situated in the limit of the sedimentary layer. Shock heating of the water-saturated sedimentary rocks typically does not produce a continuous melt sheet. We need to recalculate the shock attenuation for the specific geology of the Puchezh-Katunki structure to estimate the possible melting in the basement rocks.

One of the most interesting problems relates to the rock deformation history during complex crater formation. In the case of the Puchezh-Katunki structure one can use the level of shock metamorphism of target rocks as a "label" that marks specific points of the target. For an estimated projectile energy, the pressure attenuation curve gives the initial length of a vertical column (of 3 km at the symmetry axis) bounded by the shock pressure 45 GPa and 10 GPa. When the transient cavity reaches a maximum depth, the column seems to be shortened to approximately 1 km.

Numerical simulation of the transient crater collapse has been done using several models of rock rheology during collapse. Results show that the column at the final position beneath the central mound is about 5 km in length. This value is close to the shock-pressure decay observed along the drill core. Further improvement of the model needs to take into account the blocky structure of target rocks revealed by drilling.

The model of collapse allows the estimation of the final position of variously shocked and heated target rocks and the construction of a thermal model of the subcrater space. The comparison of observed

475185  
538-46 N93-10150  
GU586701  
VN418152  
51266589